

Control and Local Stability Analysis of a DC-DC Converter Feeding Distributed Power Systems

A. Hadri-Hamida

LEC Laboratory, Department of electrical engineering
University Mentouri-Constantine
25000, Constantine
Algeria
am_hadri@yahoo.fr

S. Zerouali, A. Allag

LMSE Laboratory, Department of electrical engineering
University Mohamed Khider-Biskra
BP 145, 07000, Biskra
Algeria
Sakina_z@yahoo.fr

Abstract – In this paper a detailed analysis is undertaken to explore the stability and bifurcation pattern of the nonlinear phenomena in the Buck DC-DC converter leading to a better understanding of its dynamics. First a nonlinear system modelling is derived for open-loop Buck converter. This model is then extended for the closed-loop system implementing a proportional - integral (PI) compensation scheme. After the initial analysis of this converter and stability region identification, we utilize the MATLAB package to analyze the detailed bifurcation scenario as the parameters are varied. The simulation was performed to achieve satisfactory dynamic performance. Finally, we propose a sliding mode controller for the proposed converter. The main goal of the control system is to regulate the output voltage and to eliminate the high current ripples.

Keywords: DC-DC converters, Chaotic systems, Sensitivity, Bifurcation, Local stability, Sliding mode control

I. INTRODUCTION

One of the requirements for the next generation of power supplies for distributed power systems (DPS) is to achieve high power density with high efficiency.

In the traditional front-end converter based on the two-stage approach for high-power three phase DPS, the DC-link voltage coming from the power factor correction (PFC) stage penalizes the second-stage DC-DC converter [1]. This DC-DC converter not only has to meet the characteristics demanded by the load, but also must process energy with high efficiency, high reliability, high power density and low cost [2].

In its simplest terms, the operation of a DC-DC converter can be described as an orderly repetition of a fixed sequence of circuit topologies. The conversion function of the converter is determined by the constituent topologies and the order in which they are repeated. Such toggling between circuit topologies is achieved by placing switches at suitable positions and turning them on and off in such a way that the required topological sequence is produced [3].

Clearly, the absence of a fixed circuit configuration poses a serious problem to the analysis and modelling of DC-DC converters. The major difficulty lies in the fact that the manner in which the system operates is highly nonlinear [4].

In most of the above investigations, sampled-data models or maps of the converters have been derived, and the bifurcation structures have been investigated with the

discrete models. Bifurcation denotes for a change in the number of candidate operating conditions of a nonlinear system when a parameter is quasi-statically varied [5]. The candidate operating condition is also an equilibrium point, a periodic solution, or other invariant subset of its limit set, without regard to its stability properties. The parameter being varied is referred to as the bifurcation parameter. A nonlinear dynamical system can exhibit many different kinds of bifurcations as one or more parameters are varied [6].

Using an exact formulation based on nonlinear maps [7], we develop a systematic method to model DC-DC converters operating with a feedback control. We use this methodology to investigate the fast-scale instabilities of a high-frequency voltage-mode buck converter [8]. Two controllers are designed. The first is based on conventional P and PI controller, the second is based on sliding mode control.

To improve the performances of the Buck DC-DC converter, a nonlinear control strategy based on sliding mode is proposed, which gives the good performance robust to disturbances as well as the fast transient responses.

The sliding mode control (SMC) is one of the popular strategies to deal with uncertain control systems [9]. The main feature of SMC is the robustness against parameter variations and external disturbances. Various applications of SMC have been conducted, such as robotic manipulators, aircrafts, DC motors, chaotic systems, and so on [10].

In this paper, a sliding mode controller is applied to the Buck DC-DC converter. It is shown via simulation results that the proposed controller has high performance both in the transient and in the steady state operations. A good control of the output voltage is obtained.

II. MODELLING OF THE BUCK DC-DC CONVERTER

A power circuit of the Buck DC-DC converter is introduced in figure 1. It consists of T_r , a controlled switch (IGBT), D , an uncontrolled switch (diode), L , an inductor, C , a capacitor and R , a load resistance. The switching of T_r is controlled by the pulse width modeling (PWM) feedback logic. The output voltage is controlled by comparing it with a reference voltage and using the error to adjust the duty ratio α . Normally, the duty ratio is obtained by comparing the error or control voltage U_c with a fixed-frequency saw-tooth voltage V_{tr} . When U_c is greater than V_{tr} the switch is turned on, and consequently the diode is turned off. When U_c is less

than V_{tr} the switch is turned off, and as a result the diode is turned on. In this case, the duty ratio in the n^{th} cycle is the solution of

$$U_c(r(k)T) = V_{tr}(r(k)T) \quad (1)$$

To derive a state-space representation for this converter operating in the continuous conduction mode with fixed-frequency duty-ratio control, we first treat the open loop system as a multi-topological system with two-circuit configurations. Each configuration describes the system in a sub-interval of time within the switching cycle T .

Hence, the period of each switching cycle can be divided into two time intervals: t_1 and t_2 , where $t_1 = \alpha T$ and $t_2 = T - t_1$. During t_1 , the switch is on and the diode is off, and during t_2 , the switch is off and the diode is on. In this model we assume that the diode and the switch are ideal. The inductor of the power stage has an equivalent series resistance r_L and the capacitor has an equivalent series resistance r_C . The inductor current is i_L and the output capacitor voltage is V_C . The topological sequence of the Buck converter consists of two linear time-invariant systems described by:

Mode 1: $0 \leq t < t_1$

The inductor current ramps up during this mode of operation which is described by the following state-space equations:

$$\begin{cases} \dot{x} = A_1^o x + B_1^o V_e \\ V_s = C_1^o x \end{cases} \quad (2)$$

where $x = [i_L, V_C]^T$, V_s is the sum of V_C and the voltage drop across r_C , V_e is the input voltage and the matrices A_1^o, B_1^o, C_1^o are given by:

$$A_1^o = \begin{bmatrix} -\frac{1}{L} \left(r_L + \frac{r_C \times R}{r_C + R} \right) & -\frac{1}{L} \left(\frac{R}{r_C + R} \right) \\ \frac{R}{C \times (r_C + R)} & -\frac{1}{C \times (r_C + R)} \end{bmatrix}, \quad B_1^o = \begin{bmatrix} 1 \\ 0 \end{bmatrix},$$

$$C_1^o = \begin{bmatrix} \frac{r_C \times R}{r_C + R} & \frac{R}{r_C + R} \end{bmatrix}$$

Mode 2: $t_1 \leq t < t_2$

During this time, the inductor current falls and the system is described by the following state-space equations:

$$\begin{cases} \dot{x} = A_2^o x + B_2^o V_e \\ V_s = C_2^o x \end{cases} \quad (3)$$

where the matrices A_2^o, B_2^o, C_2^o are given by:

$$A_2^o = \begin{bmatrix} -\frac{1}{L} \left(r_L + \frac{r_C \times R}{r_C + R} \right) & -\frac{1}{L} \left(\frac{R}{r_C + R} \right) \\ \frac{R}{C \times (r_C + R)} & -\frac{1}{C \times (r_C + R)} \end{bmatrix}, \quad B_2^o = \begin{bmatrix} 0 \\ 1 \end{bmatrix},$$

$$C_2^o = \begin{bmatrix} \frac{r_C \times R}{r_C + R} & \frac{R}{r_C + R} \end{bmatrix}.$$

From mode 1 and mode 2 we deduce the following large-signal continuous-time system by taking the averages of the intervals and summing the results:

$$\begin{cases} \dot{x} = (A_1^o \bar{r} + B_1^o \bar{V}_e) \bar{r} + (A_2^o \bar{r} + B_2^o \bar{V}_e) (1 - \bar{r}) \\ \bar{V}_s = (C_1^o \bar{r} + C_2^o (1 - \bar{r})) \bar{x} \end{cases} \quad (4)$$

Using the average model (4), we plot in figure 2 the inductor current and the capacitor voltage respectively. The solution of (2) and (3) is a discrete-time difference equation, which can be written in state-space form as:

$$x(k+1) = e^{A_1^o (1-r)T} e^{A_1^o r(k)T} x(k) \quad (5)$$

$$+ \begin{bmatrix} e^{A_2^o (1-r)T} (e^{A_1^o r(k)T} - I) (A_1^o)^{-1} B_1^o \\ + (e^{A_2^o (1-r)T} - I) (A_2^o)^{-1} B_2^o \end{bmatrix} V_e(k)$$

$$V_s(k+1) = C_2^o x(k+1) \quad (6)$$

Now, we introduce a PI controller which has this transfer function:

$$G_{contr}(p) = K_p \frac{1 + p.T_i}{p.T_i} \quad (7)$$

where K_p and T_i are the parameters of the PI controller.

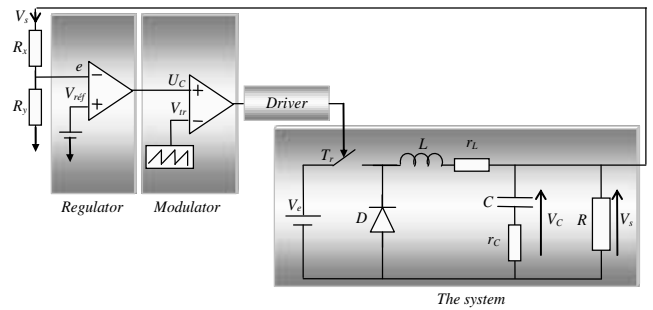


Fig. 1. Closed-loop buck regulator system with conventional P controller.

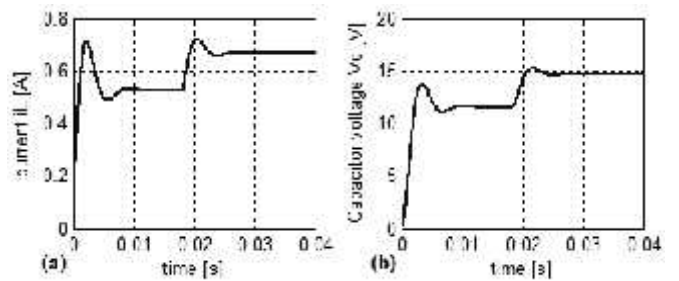


Fig. 2. (a) Inductor current i_L , (b) Output capacitor voltage V_C .

III. STABILITY ANALYSIS

The Buck DC-DC converter, presented in figure 2, employs a voltage feedback control loop. We plot in figure 3 the loop gain of the closed loop regulator system (with a proportional controller) for different values of the controller gain. The worst phase margin is 43° , and hence the converter is stable according to the small-signal averaged model. In figure 4(a), we show the bifurcation diagram where the bifurcation parameter is the controller gain. When $H_G < 8.4$, where H_G is the controller gain, the eigenvalues are inside the unit circle and hence the period-one solution is stable. As H_G is increased beyond 8.4, one of the Floquet multipliers exits the unit circle through -1, indicating a period doubling bifurcation. Consequently, the period-one solution loses stability and the period of the response is doubled. After the period-doubling bifurcation the periodic 2 orbit directly bifurcates into a chaotic orbit.

Next, we present in figure 4(b) the bifurcation diagram, which is obtained by increasing the value of the resistance load R from 10Ω to 35Ω . Initially, the period-one orbit of the closed loop system is stable. When $R = 18 \Omega$, the period-one orbit becomes unstable and a stable period-two orbit emerges. The period-doubling bifurcation was ascertained by computing the Floquet multipliers of the map. When $R = 27 \Omega$, the period-two orbit becomes unstable and a chaotic attractor emerges. We observe three important points. First, the averaged model does not predict the fast-scale instability as R , H_G , and V_e are varied, whereas the nonlinear analysis does at $R = 22 \Omega$, $H_G = 8.4$, and $V_e = 15V$.

Second, the bifurcation analysis predicts the dynamics of the system beyond the period-one instability. It shows a clear path to chaos. We note that the bifurcation diagrams in figures 4(a), 4(b), and 4(c) are obtained for a P controller. Finally, we see from figures 4(a), 4(b), and 4(c) that, even when the system response is chaotic, the ripple amplitude is not high.

IV. SLIDING MODE CONTROL

Control applications of Buck DC-DC converters have been widely investigated [11]. The main objective of research and development in this field is always to find the most suitable control method to be implemented in various DC-DC converter topologies.

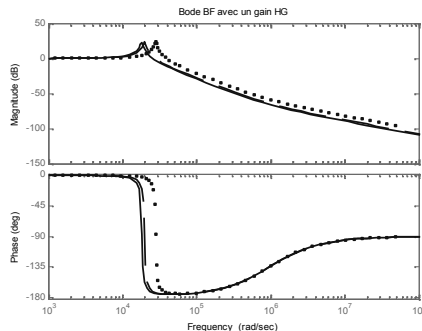


Fig. 3. Frequency-response analysis $V_e = 37V$ and $H_G = 8$ (-), 10 (--), 20 (.)

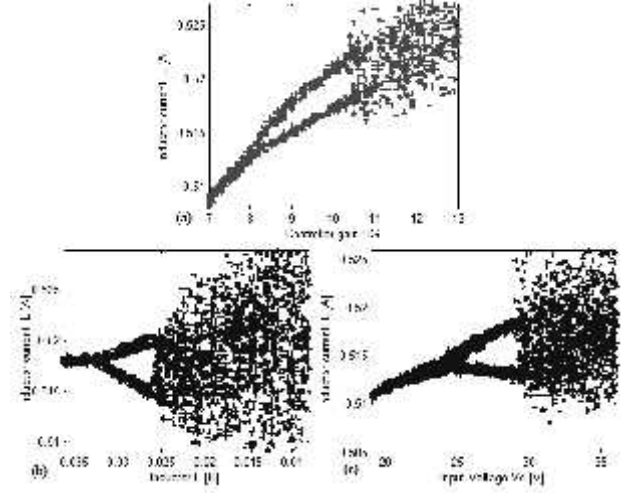


Fig. 4. Bifurcation diagrams, (a) H_G is the bifurcation parameter, (b) L is the bifurcation parameter, (c) V_e is the bifurcation parameter.

In other words, the goal is to select a control method capable of improving the efficiency of the converter, lessening the effect of electromagnetic interference (EMI), and being less effected by component variation which is the main objective in this work. The bloc scheme in figure 5 gives the configuration of the Buck DC-DC converter which utilizes a controller based on a sliding mode control law. In sliding mode control, the trajectory of the system is constrained to move or slide along a predetermined hyper plane in the state space (figure 6. (a) & (b)). Such mode is completely robust and independent of parametric variations and disturbances [12].

By eliminating the parasitic effect of the capacitor ($r_C = 0$), The system is described by the following state-space equations:

$$\dot{x} = F(x) + G(x, V_e) T_R \quad (8)$$

where T_R is the switching function which can equal to 1 or 0, and the matrices F and G are given by:

$$F(x) = \begin{bmatrix} -\frac{r_L}{L} i_L - \frac{1}{L} V_C \\ \frac{1}{C} i_L - \frac{1}{RC} V_C \end{bmatrix}, \quad G(x, V_e) = \begin{bmatrix} \frac{V_e}{L} \\ 0 \end{bmatrix} \quad (9)$$

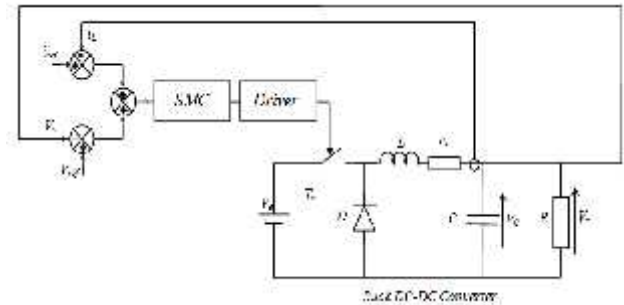


Fig. 5. Closed-loop Buck DC-DC converter with a sliding mode controller.

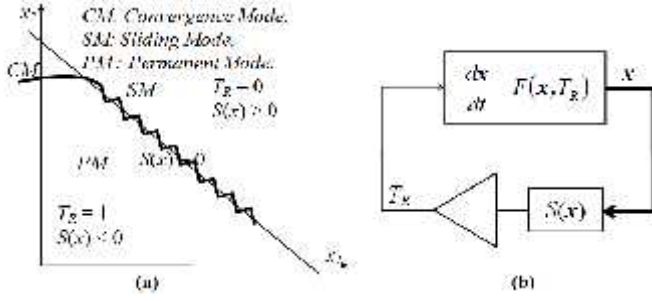


Fig. 6. (a). Trajectory modes in the state space, (b). Structure used of the SMC.

The general form of sliding surface which guarantees the convergence of the state x to its reference is given as follows:

$$S(x) = \left(\frac{d}{dt} + \lambda_x \right)^{r-1} e(x) \quad (10)$$

where r is the degree of the sliding surface and λ is a strictly positive constant. It is the first convergence condition which permits dynamic system to converge towards the sliding surfaces. It is a question of formulating a positive scalar function $V(x) > 0$ for the system states variables which are defined by the following Lyapunov function:

$$V(x) = \frac{1}{2} S(x)^T S(x) \quad (11)$$

$$\dot{V}(x) < 0 \Rightarrow S(x)^T \dot{S}(x) < 0 \quad (12)$$

Now, to define the control algorithm, it contains two terms, first for the exact linearization, the second discontinuous one for the system stability.

$$T_R(t) = T_{R_{eq}}(t) + T_{R_s}(t) \quad (13)$$

where $T_{R_{eq}}(t)$: is calculated starting from the expression $S(x) = 0 \Rightarrow \dot{S}(x) = 0$ and $T_{R_s}(t)$ is calculated from equation (12), it is given to guarantee the attractivity of the variable to be controlled towards the commutation surface.

A. Synthesis of the sliding mode controller

The sliding surfaces are given by the following expression:

$$S = e(V_s) + e(i_L) = V_{ref} - H_v V_s + i_{ref} - H_i i_L \quad (14)$$

where H_v and H_i are the sensor gains for the output voltage and the inductor current respectively. And consequently, their derivatives are given by:

$$\dot{S} = E(x) + Q T_R + W I_s \quad (15)$$

Where $x = [i_L \quad V_C]^T$, $E = \left(\frac{H_i r_L}{L} - \frac{H_v}{C} \right) i_L + \frac{H_i}{L} V_C$,

$$Q = -\frac{H_i}{L} V_c, \text{ and } W = \frac{H_v}{C}$$

we define the equivalent and the stabilizing controls respectively as:

$$T_{R_{eq}} = -Q^{-1} (E(x) + W I_s), \quad T_{R_s} = K \text{sign}(S)$$

where K is a positive constant. Finally, the control law is given by:

$$\dot{T}_R = -Q^{-1} (E(x) + W I_s) + K \text{sign}(S) \quad (16)$$

V. SIMULATION RESULTS

Figure 7 (1-5) shows the steady-state waveforms of the closed-loop system (with a PI controller) with $V_e = 18, 21, 24,$ and $40V$, respectively. The two-dimensional projections of the phase portraits on the i_L - V_C plane corresponding to these four cases are also shown (figures 7 (4)). They demonstrate clearly the period 1, period 2, period 3, and chaotic orbits. The power spectrum density for each of these cases is also shown (figures 7 (5)). We note that in the case of period 1, appears in the current spectrum an harmonics series of frequency $k * f$ such as k is an entire number, on the other hand, in the case of period 2, the spectrum of the current is enriched with a new series of harmonics of frequency $(k + 0.5) * f$. In period 3, another series of harmonics of frequency $(k / 3) * f$ appears in the spectrum of the current. Whereas, the chaos is appear by the absence of an ordered series of harmonics.

The bifurcation diagram for the system (where V_e is the bifurcation parameter) with a PI controller is shown in figure 7 (1). It is clear that the operation is stable for the input voltage chosen. However, increasing the input voltage by only $0.01V$, we find that the instability appears for low input voltages ($< 24 V$). Hence, as shown from the results for the PI controller case (figure 8 (a)), high frequency instability does exist in voltage-mode regulators.

The existing averaged-time techniques widely used in the analysis and design of voltage-mode regulators neglect this high frequency effect and as a result give an incomplete stability prediction of the regulator system.

The sliding mode controller is verified by detailed using MATLAB. A Buck DC-DC model is developed to simulate a switch-on and change load transient conditions, with the control scheme in figure 5. In figure 8 (b), we show the bifurcation diagram for the system with a sliding mode controller, where the load resistance is the bifurcation parameter. When the load resistance is increased, inductor current decreases, the period-one solution is stable. As R is increased beyond 19Ω , the period-one solution is still stable and the period of the response is not doubled. Note that the sliding mode controller eliminates the bifurcation of the system orbit. Figure 9 shows the different waveforms during load and input voltage change. The dynamic performance of the designed SMC controller is found to be satisfactory compared to that obtained with the conventional PI controller.

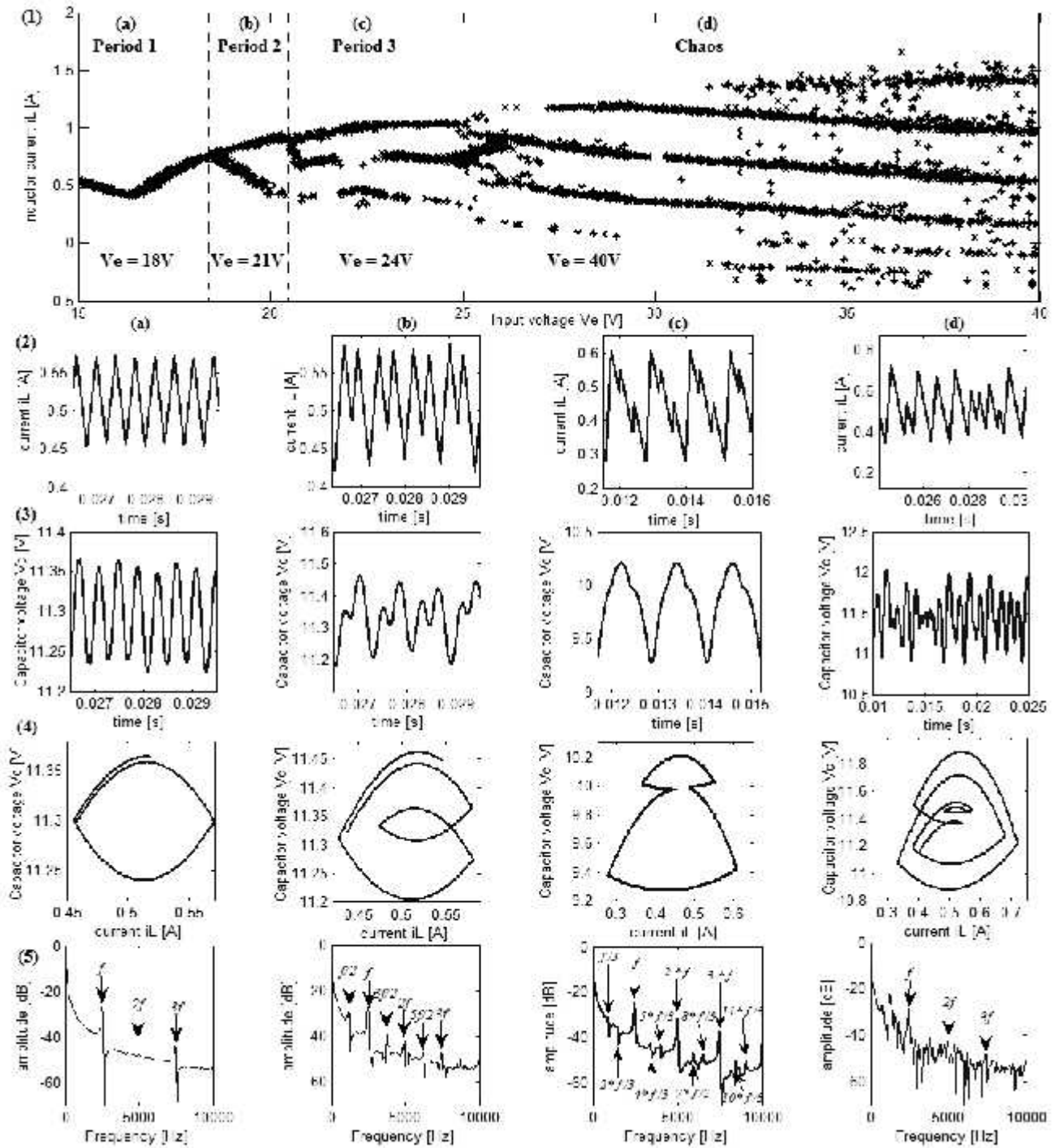


Fig. 7 (1 - 5). Bifurcation diagram where V_e is the bifurcation parameter, i_L , V_C , state plane and power spectral density of the inductor current.

VI. CONCLUSION

In this paper a nonlinear model was derived for a Buck DC-DC converter. It consists of a discrete difference equation in addition to a switching constraint.

Unlike approximate averaged or sampled-data models, this model enables the designer to investigate the behavior of the system in all regions of operation: stable and unstable.

Equilibrium solutions were calculated and their stability was investigated. Then, bifurcation diagrams were generated to study the total behavior of the system as one of its parameters varies.

Whereas the averaged model is capable of predicting the instabilities resulting from slow disturbances, it is incapable of predicting the instabilities resulting from the fast dynamics, such as subharmonics and chaos. On the other hand, using the exact nonlinear model, one can predict the instabilities resulting from slow and fast disturbances. The

exact model was used to study the stability of the Buck DC-DC converter with different compensation schemes (P, PI). Comparing the dynamic behaviors of this system, we found that instability exists in practical DC-DC converters even when the conventional design guidelines were followed.

Finally, to improve the performances of our system, we have introduced a sliding mode controller. The results show that the SMC control has fast dynamic response to external disturbances than the PI control and with the SMC control the static and dynamic performances of the output voltage are much better than with the PI control. This technique of control can reduce and sometimes eliminate the effect of load and component variation.

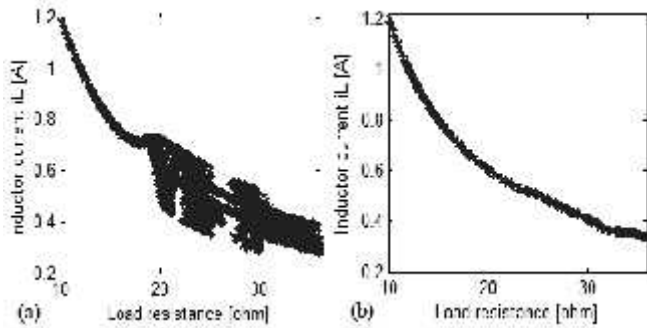


Fig. 8. Bifurcation diagram where R is the bifurcation parameter. (a) with a PI controller, (b) with a sliding mode controller.

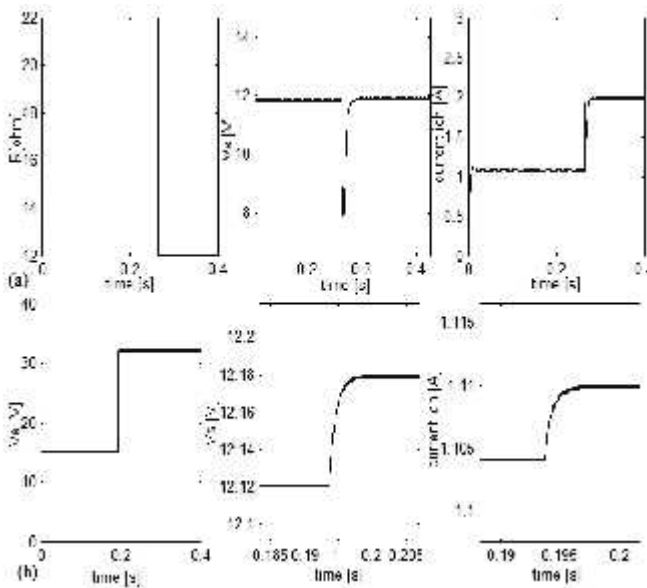


Fig. 9. Output voltage V_C , output current I_i , (a). During load change, (b). Under a step change of the input voltage.

VII. REFERENCES

[1] Hadri-Hamida A., Allag A., S. M. Mimoune, S. Zerouali and M. Feliachi, "Adaptive Nonlinear Control of a Passively Clamped Two Switch Quasi Resonant DC

Link Converter", International Journal of Applied Electromagnetic and Mechanics, vol. 25, no. 1-4, pp.537-542, ISEM Bad Gastein, IOS Press, 2007.

[2] Hadri-Hamida A., Allag A., et all. A Nonlinear Adaptive Backstepping Approach Applied to a Three Phase PWM AC-DC Converter Feeding Induction Heating. Commun Nonlinear Sci Numer Simul 2009;14(4):1515–1525.

[3] C. K. Tse and K. M. Adams, "Quasi-Linear Modeling and Control of DC/DC converters", IEEE Trans. in PE, vol. 7, no. 2, Apr. 1992, pp. 315–323.

[4] Lee, F. C., 1990, Modeling, analysis, and design of PWM converter, Virginia Power Electronic Center Publications Series, vol. 2, Blacksburg, Virginia.

[5] Nayfeh AH, Harb A, Chin C. Bifurcations in a power system model. Commun Nonlinear Sci Numer Simul 1996;6 (3):497–512.

[6] S. Wiggins, "Global Bifurcations and Chaos", Springer-Verlag, 1988.

[7] J. R.Wood, "Chaos: A real phenomenon in power electronics," in Proc. IEEE Appl. Power Electron. Conf. Expo., 1989, pp. 115–124.

[8] Dong Dai, Xikui Ma, Bo Zhang, Chi K. Tse. Hopf bifurcation and chaos from torus breakdown in voltage-mode controlled DC drive systems. Chaos, Solitons & Fractals, 2009; 41 (2): 1027-1033.

[9] A. Pisano, E. Usai. Sliding mode control: A survey with applications in math. Mathematics and Computers in Simulation 2011;81 (5):954–979.

[10] H. S. Choi, Y. H. Park, Y. S. Cho and M. Lee, "Global Sliding Mode Control Improved Design for a Brushless DC Motor," IEEE Control Systems Magazine, vol. 21, 2001, pp. 27-35.

[11] Alfayyoumi, M., 1998, Nonlinear dynamics and interactions in power electronic systems, MS Thesis, Department of Electrical and Computer Engineering, Virginia Polytechnic Institute and State University, Blacksburg, Virginia.

[12] Utkin V. I., "sliding mode in control and optimization", Springer –Verlag, Berlin, 1992.

VIII. APPENDIX

TABLE I
PARAMETERS OF THE BUCK DC-DC CONVERTER

Input voltage	V_e	15 ÷ 50 V
Switching frequency	F	$3 * 10^3$ Hz
Inductance	L	$20 * 10^{-3}$ H
Output capacitor	C	47 μ F
Equivalent series resistance	r_L	0.022 Ω
Equivalent series resistance	r_C	0.022 Ω
Load resistance	R	12 ÷ 35 Ω
V_{ref}		12 V
V_{tr}		3.0 V
K_i		$14 * 10^{-3}$
K_p		0.9130